

## Tunable interference of light behind subwavelength apertures

Feng Gao, De Li, Ru-Wen Peng,<sup>a)</sup> Qing Hu, Kuang Wei, Q. J. Wang, Y. Y. Zhu, and Mu Wang

National Laboratory of Solid State Microstructures and Department of Physics, Nanjing University, Nanjing 210093, China

(Received 3 April 2009; accepted 12 June 2009; published online 7 July 2009)

We demonstrate in this letter that electromagnetic waves passing through the subwavelength apertures on a silver film interfere with each other in the airgap behind the apertures. Depending on the width of the airgap, either constructive or destructive interference occurs. It is shown that constructive interference enhances the extraordinary optical transmission and evidently improves the quality factor, whereas destructive interference weakens the extraordinary optical transmission. We suggest that our results provide a unique approach to construct plasmonic structures and devices. © 2009 American Institute of Physics. [DOI: 10.1063/1.3167821]

According to classic theory of electromagnetic wave, the transmission through an individual subwavelength aperture is very weak.<sup>1</sup> Yet the conclusion was challenged by the observations of Ebbesen *et al.*<sup>2</sup> that the extraordinary optical transmission (EOT) occurs through an array of subwavelength holes perforated on the silver film. The phenomenon originates from the interaction of surface plasmon polariton (SPP), a collective excitation of free electrons in metal film, with the lattice structure on metal film.<sup>2–5</sup> The SPP enhances the evanescent field around apertures and thus contributes to funnel light through the holes.<sup>6,7</sup> Nowadays different type of structures and devices based on SPP has been designed and fabricated.<sup>8,9</sup> The SPP-based circuits combine photonics and electronics on nanoscale, and offer potential applications in plasmonic chips, nanolithography, and biophotonics.<sup>10</sup> However, it remains challenging to fabricate plasmonic devices in which the interaction of electromagnetic waves is tunable.<sup>11</sup> We anticipate that the tunable plasmonic devices could provide much flexibility in engineering SPP-based all-optical circuits.

In this letter, we demonstrate that interference of light can be tuned in the airgap behind the array of subwavelength holes perforated on silver film. Enhanced by SPP, the transmitted electromagnetic fields through the apertures interfere with each other in the airgap. By changing the width of the airgap, both constructive and destructive interferences can be observed. We suggest that our observations provide a unique approach to construct plasmonic structures and devices.

The structure that we are investigating here consists of a bare upper optical glass (OG) and a bottom OG coated with silver film, on which an array of nanoapertures has been fabricated. The upper and bottom glass plates are separated by an air gap. The width of the gap can be mechanically tuned by applying a pressure. The silver film on the bottom OG is blanket deposited by magnetron sputtering and the thickness is controlled to 100nm. The array of apertures is milled by focused-ion-beam (FIB) facility (strata FIB 201 from FEI, 30 keV Ga ions), and the spatial periodicity of the square lattice is  $p \cong 600$  nm, and diameter of each aperture is  $a \cong 150$  nm, as shown in Fig. 1(a). As schematically illus-

trated in Fig. 1(b), the optical transmission spectrum of the structure is measured by a UV-visible-NIR microspectrophotometer (CRAIC QDI2010). The incident light is focused on the bottom OG, and the transmitted light is detected from the upper OG.

For comparison, we first investigate the optical transmission spectrum of a structure *without* an airgap, i.e., the structure contains the silver film with aperture array on bottom OG only. Figure 1(c) illustrates the measured and calculated optical transmission spectra of the silver film with an array of apertures. EOT through the array of subwavelength apertures is observed. Three-dimensional full-vector finite-difference time-domain method has been applied in the calculation transmission spectrum.<sup>12</sup> Frequency-dependent permittivity of silver is based on Lorentz–Drude model<sup>13</sup> and periodic boundary conditions are used in calculation. One may find from Fig. 1(c) that the measured spectrum fits the calculated data reasonably well. It is known that in silver film perforated with an array of subwavelength apertures, the spatial periodicity provides a compensation momentum to

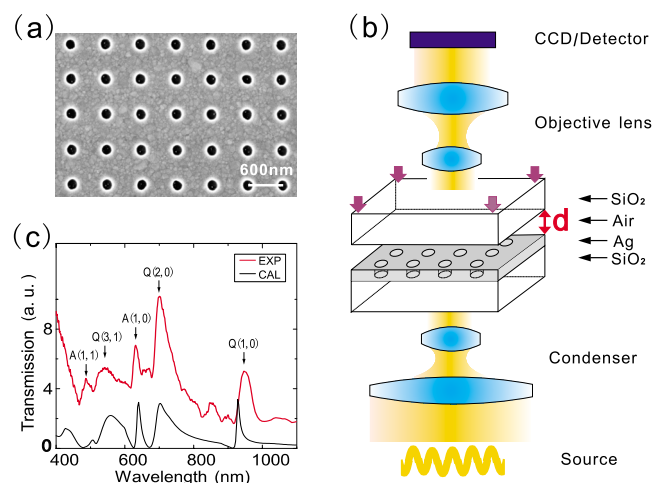


FIG. 1. (Color online) (a) The field-emission scanning electron micrograph of the array of apertures perforated on 100-nm-thick silver film. The period of apertures in the square lattice is  $p \cong 600$  nm and the diameter of the aperture is  $a \cong 150$  nm. (b) The schematics to show the experimental setup for optical measurements. (c) The measured and calculated optical transmission spectra of the structure without an airgap. The major transmission peaks have been indexed by two integers.

<sup>a)</sup> Author to whom correspondence should be addressed. Electronic mail: rwpeng@nju.edu.cn.

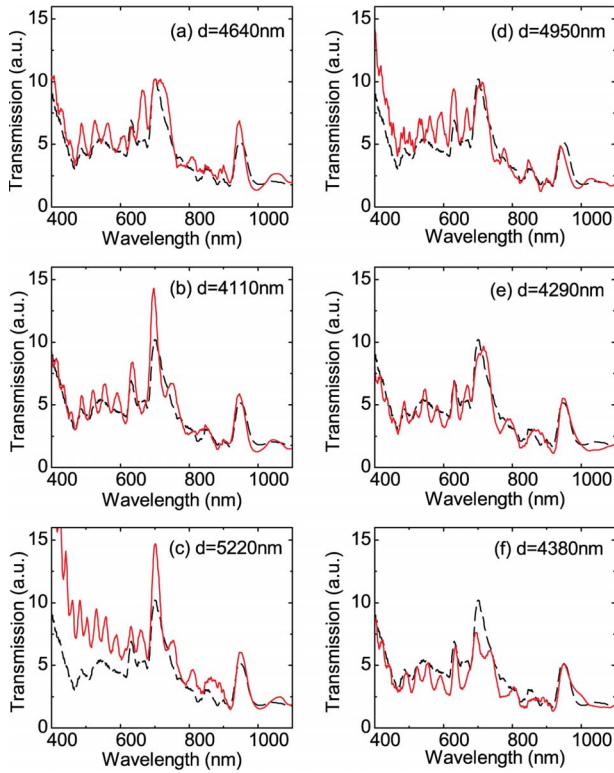


FIG. 2. (Color online) The measured transmission spectra of the structure with a tunable airgap. The width of the airgap separation in each scenario is: (a)  $d=4640$  nm; (b)  $d=4110$  nm; (c)  $d=5220$  nm; (d)  $d=4950$  nm; (e)  $d=4290$  nm; and (f)  $d=4380$  nm, respectively. The red solid lines represent the results from the structure with an airgap and the black dashed lines stand for the data without an airgap. Constructive interference occurs in cases of [(b) and (c)]; destructive interference occurs for [(e) and (f)]; and the interference just slightly modifies EOT in the cases of [(a) and (d)].

couple the incident light with SPPs on metal surface, which leads to the maximum transmission at  $\lambda_{\max} = p / \sqrt{i^2 + j^2} \sqrt{\epsilon_D \epsilon_{\text{eff}} / (\epsilon_D + \epsilon_{\text{eff}})}$ , where  $\epsilon_D$  is the permittivity of the dielectric and  $\epsilon_{\text{eff}}$  is the effective permittivity of metal with apertures,<sup>5</sup>  $i$  and  $j$  are integers. The major transmission peaks originate from the SPPs on both interfaces of air-silver and  $\text{SiO}_2$ -silver in resonance with the lattice structure. As illustrated in Fig. 1(c), the major transmission peaks are indexed respectively as  $A(1,0)$  at 635 nm,  $A(1,1)$  at 491 nm ( $A$  stands for SPP at the air-silver interface);  $Q(1,0)$  at 935 nm,  $Q(2,0)$  at 703 nm, and  $Q(3,1)$  at 556 nm ( $Q$  stands for SPP at the  $\text{SiO}_2$ -silver interface).

By introducing an airgap with tunable width ( $d$ ) behind the apertures, as that shown in Fig. 1(b), the transmitted electromagnetic fields through the apertures interfere with each other in the airgap. The measured optical transmission spectra show that as the width of airgap varies, constructive interference enhances the EOT further [as shown in Figs. 2(b) and 2(c)], and destructive interference weakens the EOT [as shown in Figs. 2(e) and 2(f)]. More specifically, interference of light behind the apertures leads to three different scenarios depending on the width of airgap  $d$ . (i) for scenarios  $d=4640$  nm and  $d=4950$  nm, the interference is weak and the intensity of EOT does not change significantly [as shown in Figs. 3(a) and 3(d)]; (ii) for scenarios  $d=4110$  nm and  $d=5220$  nm, constructive interference becomes evident, thus the intensity of EOT increases dramatically [as shown in Figs. 3(b) and 3(c)]; (iii) for scenarios  $d=4290$  nm and

$d=4380$  nm, destructive interference dominates, thus the intensity of EOT decreases obviously [as shown in Figs. 3(e) and 3(f)]. Comparing with the main peaks of EOT in the scenario without an airgap, by introducing an airgap, the positions of the transmission peaks are not changed. However, constructive interference significantly enhances the quality factor of the peak, where the quality factor is defined as  $Q = \lambda_0 / \Delta\lambda$ ,  $\lambda_0$  is the wavelength of the peak, and  $\Delta\lambda$  is the half width of the peak. For example, the quality factor of the peak indexed by  $Q(2,0)$  at 703 nm has been doubled by introducing an airgap of  $d=5220$  nm.

In order to show the physical processes for the interference of light behind the apertures, we calculate respectively the airgap-width-dependent transmission spectra, the density distributions and the phase shifts of the electric field for different resonant modes. For instance, for  $d=4190$  nm, the intensity of EOT dramatically increases for the resonant mode  $Q(2,0)$  ( $\lambda_0 \cong 703$  nm), as shown in Fig. 3(a); whereas for  $d=4370$  nm, the intensity of EOT decreases at the same mode, as shown in Fig. 3(b). The calculated transmission spectra [Figs. 3(a) and 3(b)] are in good agreement with the measurements [Figs. 2(b) and 2(f)]. The mechanism of this phenomenon can be understood as follows. When light illuminates the structure from bottom, SPP is excited on the  $\text{SiO}_2$ -silver surface ( $z=0$ ) and mainly locates around the apertures. Later, SPP is excited on the air-silver interface ( $z \cong 100$  nm). SPP enhances the evanescent field at the apertures [as shown in Figs. 3(c) and 3(d)]. From silver top surface ( $z \cong 100$  nm) up to the region of  $z \cong 300$  nm, the evanescent field around aperture decays gradually, yet the electromagnetic field on silver film increases [as shown in Figs. 3(e) and 3(f)]. (Please note the evanescent field around aperture is much stronger than the field on the top surface of silver film,  $z=100$  nm.) In the region from  $z \cong 300$  nm to  $z \cong 600$  nm, both of these fields are coupled and transmitted upward. The transmitted field is reflected by the upper OG and then multiple reflected between the top surface of silver and the surface of the upper OG. Therefore, interference occurs in the airgap between the top surface of silver and the bottom surface of the upper OG. Based on rigorous coupled-wave analysis method,<sup>14</sup> we calculate the zero-order reflectance at air-silver surface for mode  $Q(2,0)$  at  $\lambda_0 \cong 703$  nm. It turns out that the interference is constructive when the phase shift  $\Delta\phi$  of electric field satisfies  $n\pi - 0.13\pi < \Delta\phi < n\pi + 0.3\pi$  through the airgap; whereas it becomes a destructive interference when the phase shift of electric field satisfies  $n\pi + 0.3\pi < \Delta\phi < n\pi + 0.87\pi$ ; the interference does not change significantly when the phase shift of electric field is around  $\Delta\phi = n\pi - 0.13\pi$  or  $\Delta\phi = n\pi + 0.3\pi$  ( $n$  is an integer). For example, zero phase shift of electric field occurs at  $d=4190$  nm [Fig. 3(g)], thus interference is constructive and the resonant mode  $Q(2,0)$  of EOT is enhanced behind the apertures. The quality factor of transmission peak is also increased due to multiple scatterings. When the phase shift of electric field is about  $\pi/2$  [Fig. 3(h)] and the airgap separation is  $d=4370$  nm, destructive interference takes place, and resonant mode  $Q(2,0)$  of EOT is decreased behind the apertures.

To summarize, we demonstrate in this letter that tunable interference of light occurs in an airgap behind the array of subwavelength apertures perforated on silver film. SPP enhances the evanescent field at the apertures, and the transmit-

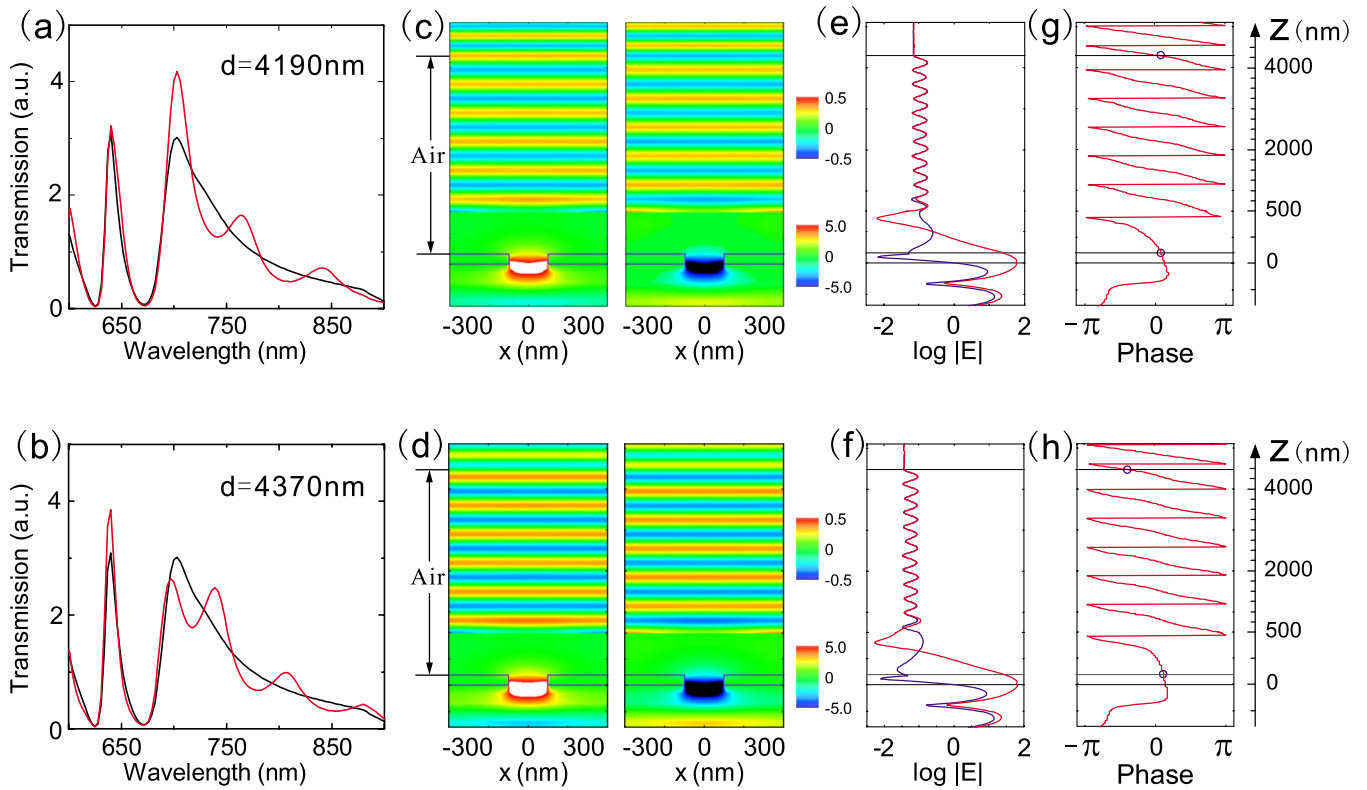


FIG. 3. (Color online) The plots to show the calculated zero-order transmission spectra, the density distributions and the phase shifts of the electric field in the structure. The upper row represents the results from the structure with airgap separation  $d=4190$  nm and the lower row shows the results from the structure with airgap separation  $d=4370$  nm. [(a) and (b)] are the calculated zero-order transmission spectra of the structures. The red line represents the result for the structure with an airgap, whereas the black line represents the result without an airgap. [(c) and (d)] are the snapshots of the field distribution of the structure for mode  $Q(2,0)$  ( $\lambda_0 \cong 703$  nm) when the intensity at the aperture ( $x=0$  and  $z=100$  nm) reaches its maximum (left) and minimum (right), respectively. [(e) and (f)] represent  $z$ -dependent electric field ( $|E|$ ) distributions in the structures. The red line represents the data at  $x=0$ , and the blue line represents the data at  $x=300$  nm. [(g) and (h)] show the  $z$ -dependent phase shift of electromagnetic wave passing through an airgap (for  $x=0$ ), compared with a free propagation wave arriving at  $z=0$ . In order to show the phase shift through the whole airgap, the phases at both the air-silver interface and the top OG are marked by the blue circles. In simulation, periodic boundary condition is set on  $x$ - $y$  plane, and absorption boundary condition is set at both  $z=5100$  nm and  $z=-900$  nm.

ted electromagnetic fields through the apertures interfere with each other in the airgap. Depending on the width of the airgap, constructive interference enhances the EOT further and increases its quality factor, whereas destructive interference weakens the EOT obviously. We suggest that our observations provide a unique approach to design tunable plasmonic structures and devices.

This work was supported by grants from the NSF of China (Grant Nos. 10625417, 50672035, and 10874068), the MOST of China (Grant Nos. 2004CB619005 and 2006CB921804), and partly by Jiangsu Province (Grant No. BK2008012).

<sup>1</sup>H. A. Bethe, *Phys. Rev.* **66**, 163 (1944).

<sup>2</sup>T. W. Ebbesen, H. J. Lezec, H. F. Ghaemi, T. Thio, and P. A. Wolff, *Nature (London)* **391**, 667 (1998).

<sup>3</sup>L. Martín-Moreno, F. J. García-Vidal, H. J. Lezec, K. M. Pellerin, T. Thio, J. B. Pendry, and T. W. Ebbesen, *Phys. Rev. Lett.* **86**, 1114 (2001).

<sup>4</sup>C. Genet and T. W. Ebbesen, *Nature (London)* **445**, 39 (2007).

<sup>5</sup>Z. H. Tang, R. W. Peng, Z. Wang, X. Wu, Y. J. Bao, Q. J. Wang, Z. J. Zhang, W. H. Sun, and M. Wang, *Phys. Rev. B* **76**, 195405 (2007).

<sup>6</sup>H. Liu and P. Lalanne, *Nature (London)* **452**, 728 (2008).

<sup>7</sup>Y. J. Bao, R. W. Peng, D. J. Shu, M. Wang, X. Li, J. Shao, W. Lu, and N. B. Ming, *Phys. Rev. Lett.* **101**, 087401 (2008).

<sup>8</sup>W. L. Barnes, A. Dereux, and T. W. Ebbesen, *Nature (London)* **424**, 824 (2003).

<sup>9</sup>N. Fang, H. Lee, C. Sun, and X. Zhang, *Science* **308**, 534 (2005); Z. J. Zhang, R. W. Peng, Z. Wang, F. Gao, X. R. Huang, W. H. Sun, Q. J. Wang, and M. Wang, *Appl. Phys. Lett.* **93**, 171110 (2008).

<sup>10</sup>E. Ozbay, *Science* **311**, 189 (2006).

<sup>11</sup>A. Battula, S. Chen, Y. Lu, R. J. Knize, and K. Reinhardt, *Opt. Lett.* **32**, 2692 (2007).

<sup>12</sup>A. Taflov and S. C. Hagness, *Computational Electrodynamics: The Finite-Difference Time-Domain Method*, 3rd ed. (Artech House, Boston, 2005).

<sup>13</sup>A. D. Rakic, A. B. Djuric, J. M. Elazar, and M. L. Majewski, *Appl. Opt.* **37**, 5271 (1998).

<sup>14</sup>L. Li, *J. Opt. Soc. Am. A Opt. Image Sci. Vis.* **14**, 2758 (1997); E. Silberstein, P. Lalanne, J. Hugonin, and Q. Cao, *ibid.* **18**, 2865 (2001).